hydrogen

MDPI

Article

High Efficiency in Clean Hydrogen Production Using Water and AlLi Phases Prepared by Mechanical Alloying

José Luis Iturbe-García [1,*] and Diana Laura Alvarez-Acosta [1,2]

[1] Departamento de Química, Instituto Nacional de Investigaciones Nucleares, Carretera México-Toluca s/n, La Marquesa, Ocoyoacac C.P. 52045, Estado de México, Mexico; dlalvareza@outlook.com
[2] Facultad de Química, Universidad Autónoma del Estado de México, Paseo Colón y Tollocan s/n, Toluca C.P. 50000, Estado de México, Mexico
* Correspondence: joseluis.iturbe@inin.gob.mx; Tel.: +52-5553297200 (ext. 12274)

Abstract: In this work, the results of clean hydrogen production from the direct chemical reaction between aluminum–lithium compounds and distilled water under normal conditions, without additives or catalysts, are presented. The material was prepared by mechanical alloying using a high-energy Spex-type mill in an Al20Li ratio. Relatively short milling times were programmed for the preparation of AlLi phases. Through this process, two phases (AlLi and Al8.9Li1.1) were identified, which react efficiently to produce clean hydrogen. The experiments demonstrate fast and self-sustained reactions between AlLi phases and distilled water. In both the phase preparation and hydrogen generation, 100% efficiency was achieved. The hydrolysis reaction occurred quickly, and the hydrogen volume generated was 1700 mL/g of material. Under these conditions, aluminum generates 1390 mL of hydrogen, and lithium generates 310 mL/g from both AlLi phases. A single by-product ($LiAl_2(OH)_7{\cdot}2H_2O$) was identified. According to the results and the conditions applied in this research, the hydrogen produced does not require prior purification and can therefore be used directly in fuel cells. The AlLi–water reaction is a promising process for generating hydrogen in a simple and relatively short time compared to other hydrogen production methods. In this process, no greenhouse gas emissions were produced.

Keywords: AlLi phases; mechanical alloying; hydrolysis; hydrogen; lithium aluminum hydroxide

Citation: Iturbe-García, J.L.; Alvarez-Acosta, D.L. High Efficiency in Clean Hydrogen Production Using Water and AlLi Phases Prepared by Mechanical Alloying. *Hydrogen* **2024**, *5*, 987–1003. https://doi.org/10.3390/hydrogen5040053

Academic Editors: Aleksey A. Vedyagin and Adolfo Iulianelli

Received: 28 August 2024
Revised: 27 November 2024
Accepted: 3 December 2024
Published: 9 December 2024

1. Introduction

The energy economy based on fossil fuels is considered unsustainable due to the air pollution caused by the emission of large amounts of greenhouse gases (GHGs) [1]. The main inputs of global energy systems are oil, coal, and natural gas [2–4]. However, when fossil fuels or their derivatives are used in ground, marine, or air transport, large amounts of CO_2 are emitted, negatively affecting the environment. The consequences of global warming have become increasingly evident in recent years. Since 1995, this issue has been widely discussed in various scientific, political, and economic forums (Paris 2015, Bonn 2017, Egypt 2022, Dubai COP 2023). To date, significant progress has been made through agreements regarding fuel transitions, as demonstrated by some automotive companies in recent years. However, greater responsibility is required to carry out the transition from fossil fuels. This transition has already begun, as evidenced by advances in the commercialization of electric and hybrid vehicles, primarily based on hydrogen fuel cells and lithium batteries, which will gradually replace those that use fossil fuels. This transition is not easy, as it is also very expensive; but eventually, this economy will become a reality in the coming years. Therefore, it is essential to incorporate new fuels that do not generate GHGs and that are beneficial to both health and the environment. This is the main reason why scientists around the world are focusing on developing fuels that avoid GHG emissions and can meet current and future global energy demands while mitigating environmental degradation. The search for new energy sources is primarily

focused on hydrogen technology. Hydrogen is a renewable, environmentally friendly fuel with a high calorific value and is an important energy carrier that could play a fundamental role in reducing GHG emissions [5,6]. Today, the best-known technologies for hydrogen production include natural gas reforming, bio-derived liquid reforming, coal gasification, water electrolysis, thermochemical, photoelectrochemical, and biological processes, among others [7,8]. Unconventional and more sophisticated methods, such as irradiating metals like Ti, Si, Mg, and Al, or their combinations with laser ablation to carry out hydrolysis reactions, have also been used to generate hydrogen [9,10]. Additionally, hydrogenated solvents, such as methanol, are used in hydrogen generation through various methods; methanol is particularly suitable for producing hydrogen by releasing the four hydrogen atoms in its molecule. Methanol is a substance used alone or in combination with other solvents to produce hydrogen by various methods, with or without the use of catalysts, as reported in the literature [11–17]. Another promising method for generating hydrogen is the metal–water reaction, which takes into account particle size and temperature. This method can also be applied in energy storage, and the metal oxides produced can be deoxidized and reused. This process is considered effective, safe, economical, and easy to use [18–20]. Recent research has explored the use of metals such as Al, Zn, and Mg to generate hydrogen, with aluminum (Al) being considered the most viable candidate due to its abundance in the Earth's crust, high performance, and recyclability [21–24]. The main challenge in hydrogen production using aluminum is the efficient removal of the oxide layer that forms on its surface, which prevents the metal from easily reacting with water. Various methods, including some recent ones, have been studied to facilitate the hydrolysis of aluminum, including chemical activation of the metal, mechanical milling, and alloy formation to generate hydrogen for use in fuel cells [25–28]. These methods include combining aluminum with other metals, specifically (Ga), as well as (In), (Sn), and (Zn) or their combinations in varying percentages [29–37]. Other approaches involve the use of additives, modifying agents, or adjustments to water temperature [38,39]. Each of these processes has its own advantages and disadvantages. One disadvantage of aluminum is the formation of an oxide layer on its surface, which limits direct contact with water, making it difficult to efficiently obtain hydrogen from the reaction. Other studies have focused on minimizing this oxide layer and have proposed several effective methods for hydrogen production, such as forming Al alloys through mechanical alloying using fine particles and adding additives (alkalis, metal oxides, salts, hydrides, etc.) [40,41]. Mechanical alloying has the advantage of preventing the loss of molecules by evaporation from metals with low melting points during alloy preparation. Additionally, lithium is a highly reactive metal that can produce hydrogen when it reacts with water. Lithium can be mixed with aluminum to form AlLi alloys, which enhance the activity of aluminum. It has been reported that combining lithium with aluminum has a significant effect: As the concentration of lithium increases, the formation of LiOH also increases, accelerating aluminum hydrolysis and improving the reaction yield [42–46]. The lithium content significantly contributes to the formation of AlLi alloys, changing the AlLi compound to Al_2Li_3 and Al_4Li_9 as lithium increases from 10% to 30% or 40% by weight, respectively [47]. However, this parameter not only affects hydrogen production but also impacts mechanical alloying. A low concentration of lithium can cause particle agglomeration, and as the amount of lithium decreases, these effects become more frequent [48]. Consequently, when materials are prepared using the mechanical alloying method, it is common to add small amounts of process control agents or additives to reduce agglomeration. However, this makes the alloy composition more complex, leading to difficulties when recycling the metal. In this study, aluminum and lithium elements, with 80% and 20% by weight, respectively, were used to prepare the alloy through mechanical alloying with varying milling times and without the addition of any additives. The materials obtained reacted efficiently with distilled water under normal pressure and temperature conditions to generate clean hydrogen. These results help to understand the contribution of aluminum in the reaction of the Al20Li phases obtained through this method. For each programmed milling time, the

samples were reacted with water, and the hydrogen volume was compared. The formation of Al20Li phases was identified using XRD analysis.

2. Materials and Methods

2.1. Materials

The metals used in the preparation of the Al-Li compound were aluminum (Aldrich Chemistry, St Louis, MO, USA) in granular form, with particle sizes of approximately 1 mm and a purity of 99.7%, and lithium (Alfa Aesar, Miami, FL, USA) also in granular form, with particle sizes of 1–4 mm and a purity of 99.4%. A high-energy spex mill was used to prepare the AlLi samples, which was built at our institute in the general workshops department whose images are provided in [49]. The container and milling media are made of stainless steel and were provided by the same department. A glove box under an ultra-high purity argon (Ar) atmosphere (CRiOGAS, Purity Plus SPECIALTY GASES, Toluca, Mexico) was used for handling the metals before milling.

2.2. Sample Preparation

In each experiment, approximately 5 g of the compound in a percentage ratio of 80:20 by weight for aluminum and lithium, respectively, was prepared with a ball-to-powder ratio of 5, using three milling media, each 1.2 mm in diameter. This procedure was performed inside the glove box to avoid contact of the materials with the environment. The AlLi compounds were prepared with milling times ranging from 30 min to 3 h. In all experiments, after the mechanical alloying process, the material inside the container was passivated for 18 h to prevent spontaneous oxidation of the formed phases.

2.3. Characterization

The powders were characterized using various techniques to determine certain structural properties as well as their composition. The surface area, pore size, and micropore volume were determined by physical adsorption of N_2 at 77 K using an automatic adsorption system (BELSORP Max, Bel Japan, Inc., Osaka, Japan). Before analysis, the samples were degassed 3 h at 200 °C. The samples, both before and after milling, as well as the by-product, were characterized by X-ray diffraction. The diffractograms were collected using a Bruker D8 Advance X-ray powder diffractometer with an energy-dispersive one-dimensional detector to identify the phases formed. The samples were placed on a Lucite support and then in the goniometer of the diffractometer. Some of the parameters used in these determinations included a Kα radiation source from a Cu anode with a wavelength (λ) of 1.5406 Å, a diffracted beam monochromator set to 40 kV and 40 mA, 2θ steps of 0.02°, and programmed times of 20 min to acquire the X-ray diffraction patterns, with intensities high enough for subsequent identification. The interval used to acquire the spectrum ranged from 20 to 90 degrees in 2θ. Identification and quantification of the crystalline phases were performed using DIFFRAC.EVA and TOPAS software V7. This software is supported by a reference pattern database derived from the Crystallography Open Database (COD) and the Powder Diffraction File (PDF) for phase identification. A scanning electron microscope (JEOL 5900 LV) equipped with an energy-dispersive X-ray (EDAX) probe for microanalysis was also used to determine the morphology and chemical composition of the samples.

2.4. Hydrogen Production

For hydrogen generation, the AlLi compounds in powder form were weighed between 20 and 200 mg; for the reaction, each sample was placed in a 20 mL glass vial, sealed with a rubber stopper and an aluminum O-ring. A syringe tip was attached to a hose through which the gas passed toward a graduated burette, where the generated hydrogen was measured by liquid displacement. With another syringe, 5 mL of distilled water was added to the vial with the sample to generate hydrogen. The reactions were carried out under ambient laboratory conditions, mainly at a temperature of 20 °C, gradually

and slowly adding distilled water to control the exothermic reaction. The by-product obtained after the reaction was separated from the liquid phase and dried on a grill at a controlled temperature. The samples, both before and after milling, as well as the by-product, were characterized by X-ray diffraction. Under these same conditions, a series of reactions were performed between metallic lithium particles of known weight and distilled water to generate hydrogen, which was considered to determine the volume of hydrogen produced by aluminum from the Al-20Li phases. Figure 1 shows the diagram with different experimental stages carried out in preparation for the AlLi compound until hydrogen generation as the main objective of this work.

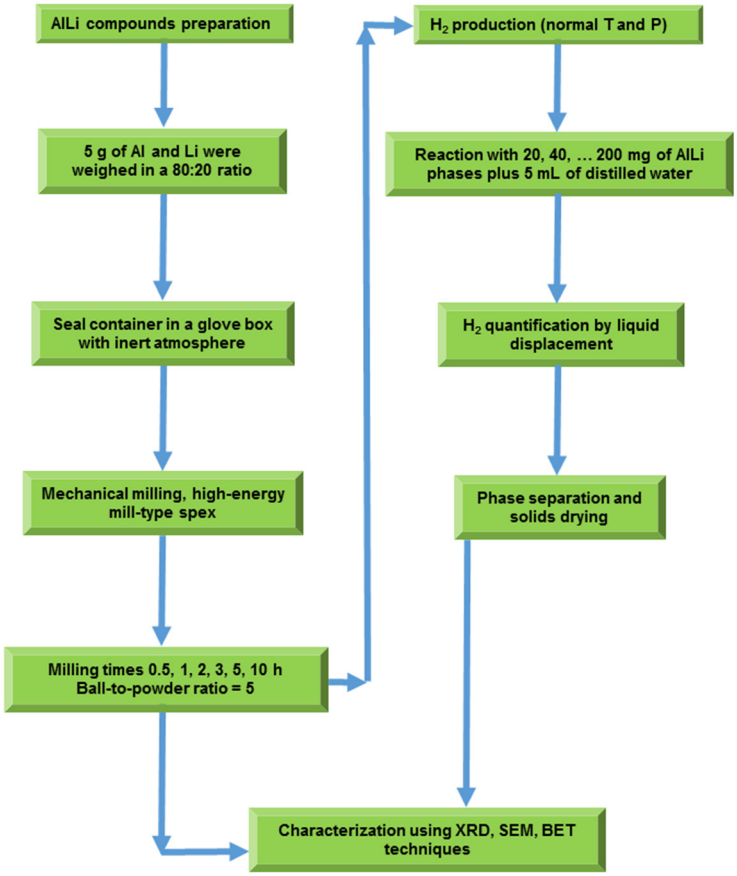

Figure 1. Experimental diagram for hydrogen generation.

3. Results and Discussion

It is important to understand the structural changes in Al and Li materials before and after milling, particularly in terms of shape and size, as they undergo significant modifications over time. These structural changes facilitate the reaction with water for hydrogen generation. Aluminum, for example, does not react directly with water to generate hydrogen due to the formation of an oxide layer. However, when combined with lithium and activated through milling, hydrolysis occurs, and hydrogen is easily generated. Figure 2A shows a micrograph of aluminum pellets used in the preparation of the AlLi compound. The image reveals particles with irregular morphology. Although the pellets appear circular and silver-colored to the naked eye, the microscopic view in the image shows their irregular form. This irregularity may be due to the preparation method, as the material lacks a specific shape. On the other hand, based on the image and the scale, the particle size is greater than 1 mm. The particles have irregularities, with one end being narrower and the opposite sides wider. The surface shows a series of overlapping plates with irregularities across all the granules. The shape of the particles may be due to the preparation method, as in some cases, this metal is synthesized by the electrolysis of molten

salts. The micrograph, with a magnification of 50X, was sufficient to observe these particles in detail. The required magnification depends on particle size—larger particles require less magnification for visualization. In this case, an electron beam with a power of 20 kV was applied. Generally, these particles show a pattern in which the thinnest part appears folded. Figure 2B shows an image of a metallic lithium granule, where some lines are visible on its surface, suggesting the particle underwent a cross-section. The front is flat, while the rest has a bumpy appearance. This material is extremely difficult to handle due to its high reactivity with the environment, particularly its rapid reaction with ambient humidity. For this reason, the lithium was carefully prepared in a glove box under an argon atmosphere to prevent any possible reaction with atmospheric components before coming into contact with water. Before analysis, the lithium samples were coated with a layer of gold to prevent electrical overcharge and to protect them from environmental exposure. This process was conducted in a vacuum. The SEM analyses were performed at 40X magnification, which was sufficient to observe the surface details due to the size of the lithium grains. Another analysis was conducted on the aluminum using the EDAX probe to determine whether any impurities were present in its structure. This analysis could only be performed on aluminum, as lithium, due to its physicochemical properties, cannot be excited to emit characteristic X-rays, making it impossible to determine its elemental composition. The EDAX analysis of the aluminum indicated the presence of a single peak corresponding to the characteristic X-ray pattern of aluminum, with no other elements detected as impurities. When working with pure elements, as in this case, there is the advantage of obtaining bimetallic alloys without the presence of any other elements, which is important because impurities can alter the properties and potential applications of the resulting compound.

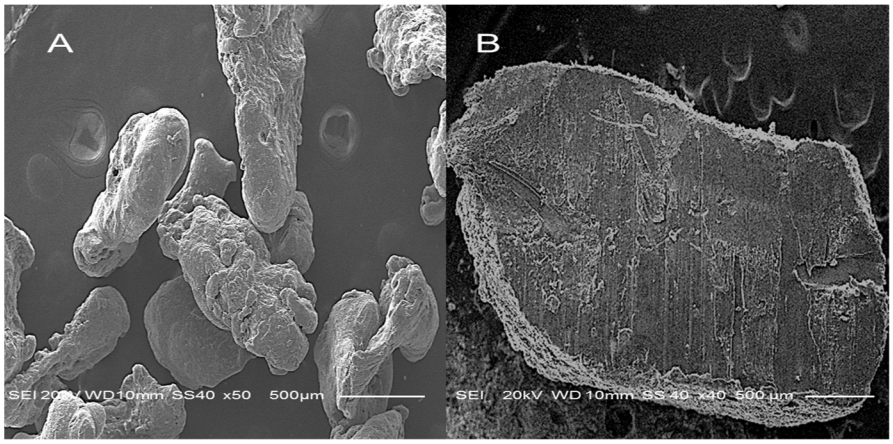

Figure 2. Micrographs of aluminum (**A**) and lithium (**B**) used in AlLi compounds' preparation.

Figure 3 shows images of the AlLi material after mechanical alloying for 30 min, 1, 2, and 3 h, A, B, C, and D respectively. Clusters, formed by small particles, were identified. Image analysis was performed at 100X magnification, providing a general view of the powders and clearly showing the physical transformation of the material, with particle sizes completely altered from the original aluminum and lithium metals (Figure 2A,B). The processing of the metals depends on the milling time, and the structural changes occurred due to the high impact between the container walls and the milling media, caused by the motion of the engine that transmits the force to the system holding the container. In Figure 3A, a significant change in the morphology and size of the starting elements (Al and Li) was observed after a short milling time (30 min). During this process, a partial fusion phenomenon occurs between these two metals, which are considered soft due to their physicochemical properties. Initial fusion happens more easily in short milling times, and under these conditions, phase formation begins to be observed. The morphological changes during the milling of these ductile powders can be explained by the competition between two mechanisms: fracture and cold welding. Impacts between the milling media and

container walls repeatedly flatten the Al and Li particles from the start of milling, resulting in cold welding and the formation of larger, flake-like particles. Plastic deformation hardens the particles, making them brittle, which activates the fracture mechanism during short milling periods, such as after 1 h, as shown in Figure 3B. Some particles retain a certain size, while others are flattened. When the milling time is increased to 2 h, a more uniform distribution is observed, and the flake-like particles undergo fracture, forming smaller particles, as shown in Figure 3C. At this stage, the fracture mechanism becomes dominant over cold welding. After 3 h of milling, the flattened particles transform into equiaxial morphology, and the particle size decreases. Under these conditions, the microstructure of the alloy is formed, consisting of globular grains where the particles have a nearly uniform size and are evenly distributed, as shown in Figure 3D. Another important factor affecting the material's transformation process is the size of the milling media. In these experiments, 12 mm diameter balls were used, subjecting the metals to high impacts at each instant within the system, which caused significant changes in their morphology. However, it is important to note that even after the particle size has stabilized, microstructural refinement can still occur and may continue later due to the thermal excitation conditions that are maintained inside the container. In the same figure, the effect of milling time on the particle sizes of Al and Li is also shown, demonstrating a complete change in their morphology. It is clear that milling for only 3 h, using large millings media, results in a significant reduction in particle size, which is favorable for hydrogen generation through reaction with water. To determine if there are any significant morphological changes beyond 3 h, milling times of 5 and 10 h were tested. According to the results, no notable changes in grain size were observed, and the globular particles had similar morphologies to those obtained after 3 h of milling, without the formation of amorphous materials (image not shown because it is similar to Figure 3D). Additionally, when the particles obtained after 3, 5, and 10 h of milling were reacted with water, the same volume of hydrogen was generated. These results indicate that the preparation of the AlLi alloy can be effectively completed with short milling times of no more than 3 h. One of the advantages of preparing metal alloys through the mechanical alloying process, unlike conventional methods, is that it does not require a large amount of energy in the form of heat. High temperatures that would melt the metals and produce vapors potentially harmful to the health of operators are avoided. Additionally, it has been demonstrated that metal alloys can be prepared in short time periods using high-energy mechanical milling, as in this case, where the material was formed from Al and Li, with alloy formation beginning after just 30 min of milling.

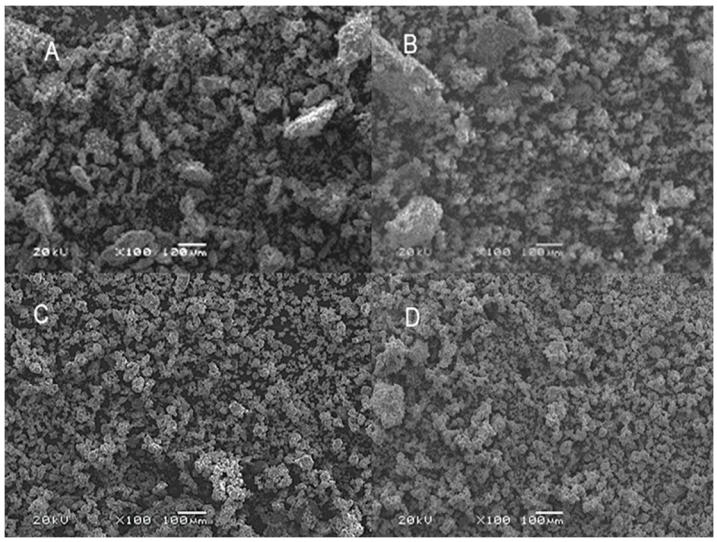

Figure 3. Micrograph of AlLi powders milled 0.5 (**A**), 1 (**B**), 2 (**C**), and 3 h (**D**).

Figure 4 shows the adsorption/desorption curves of AlLi phases A and B, respectively. The solid powders milled for 3 h were analyzed using the nitrogen physisorption technique, which provided isotherms similar to the type IV curve proposed by IUPAC, corresponding to mesoporous materials with pore sizes ranging from 2 to 50 nm. The analysis was conducted at a relative pressure (p/p_0) of 0.99, with nitrogen adsorption reporting a total pore volume of 0.69 cm^3/g for the AlLi and $Al_{8.9}Li_{1.1}$ phases prepared by mechanical milling. Using the multipoint BET method at a p/p_0 interval from 0 to 1, the specific surface area was measured at 183 m^2/g for the AlLi and $Al_{8.9}Li_{1.1}$ phases. Additionally, the average pore diameter was 15.03 nm, suggesting that the material had good porosity prior to reacting with water. The adsorption/desorption isotherm of N_2 at 77 K, presented in Figure 4, reflects the porous texture of the AlLi and $Al_{8.9}Li_{1.1}$ powders used in hydrogen generation. The isotherm is characterized by a hysteresis loop, which is associated with capillary condensation occurring in mesoporous materials and limiting uptake over a high p/p_0 range. Some mesoporous materials exhibit type IV isotherms, and in general, when their surface area is large, they have a greater capacity to adsorb gases [50,51]. The hysteresis loop found in this study was an H3 type, which does not exhibit limiting adsorption at high p/p_0. This type of hysteresis may also correspond to particle aggregates with pores of non-uniform sizes and shapes.

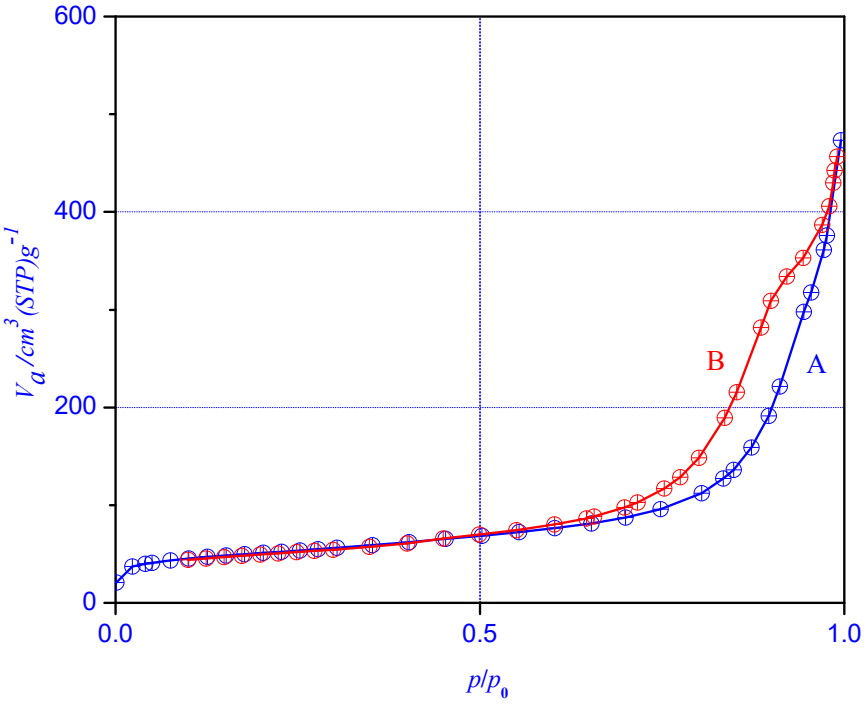

Figure 4. Nitrogen adsorption (A)/desorption (B) isotherm at 77 K of AlLi and $Al_{8.9}Li_{1.1}$ phases.

Figure 5 shows five diffraction patterns corresponding to aluminum and the compounds obtained by milling at different programmed times. It should be noted that lithium could not be characterized using X-ray diffraction due to its low atomic number. Diffractogram (a) corresponds to the aluminum particles, where five characteristic peaks appear in the range of 35 to 85 degrees in 2θ. The metal was identified using PDF card 01-1180, corresponding to the image of the particles represented in Figure 2A. The following diffractograms—(b), (c), (d), and (e)—correspond to samples with milling times of 30 min, 1, 2, and 3 h, respectively. Two phases were obtained: $Al_{8.9}Li_{1.1}$ and AlLi, identified using PDF cards 65-7533 and 65-4905, respectively. As milling time increases, the transformation of the aluminum and lithium metals into both phases (AlLi and $Al_{8.9}Li_{1.1}$) becomes evident. This same transformation was confirmed through SEM analyses, with the four images in Figure 2 corresponding to each diffraction pattern (b, c, d, and e), respectively. As milling time progresses, the size of the materials decreases, reaching micrometric structures. The

intensities of the $Al_{8.9}Li_{1.1}$ phase closely resemble those of aluminum, and they can only be differentiated using PDF cards based on their respective theoretical values. The amplified peaks also indicate the formation of the AlLi phase, which shows distinct diffraction patterns compared to aluminum, as seen in the diffractograms where the peaks are clearly separated. In the diffractogram (b), a small peak at 40.067 degrees in 2θ appears after the main peak, corresponding to the AlLi phase. This indicates that the formation of this phase had already begun after just 30 min of milling, meaning that both phases ($Al_{8.9}Li_{1.1}$ and AlLi) are present under these conditions. To confirm phase formation, each aluminum peak was compared with those of the $Al_{8.9}Li_{1.1}$ and AlLi phases, and the intensities of the various diffractograms were carefully examined.

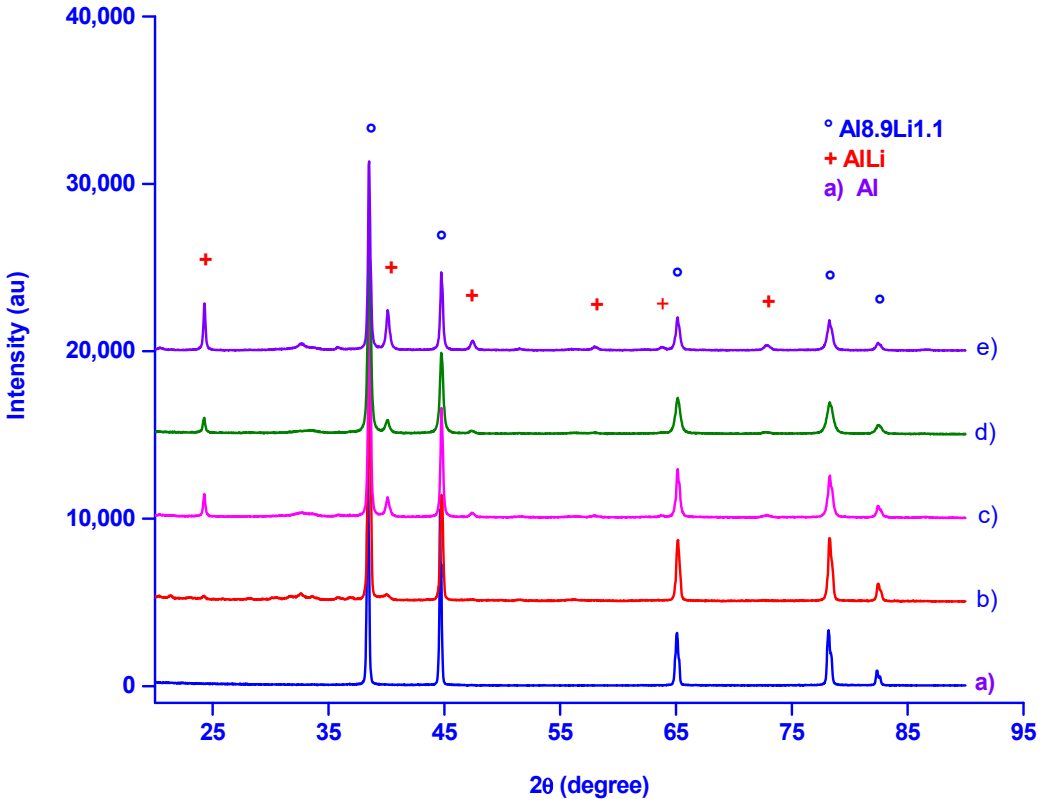

Figure 5. Diffractograms of Al (a) and ($Al_{8.9}Li_{1.1}$ and AlLi) phases after 30 min (b), 1 (c), 2 (d), and 3 h (e) of milling.

Figure 6 shows the amplified diffractograms of the main peaks of both aluminum and the $Al_{8.9}Li_{1.1}$ and AlLi phases, which vary depending on the milling time. To distinguish the aluminum spectrum from that of the $Al_{8.9}Li_{1.1}$ phase, peak broadening was performed. The figure provides a detailed comparison, focusing on the range from 33 to 44 degrees in 2θ. As seen in all diffractograms (Figure 5), there is a strong similarity between the intensities of aluminum and the $Al_{8.9}Li_{1.1}$ phase, making a comparison of the five peaks from both compounds necessary. Upon expanding each peak, all displayed slight displacements, which were corroborated with their respective theoretical values. In the diffractograms, the two main peaks of both aluminum (a) and the $Al_{8.9}Li_{1.1}$ phase were analyzed. According to theoretical values, the 2θ angle of 38.610 corresponds to the main peak of aluminum, while the main peak of the $Al_{8.9}Li_{1.1}$ phase is at 38.506. This results in a difference of 0.104 degrees between the two values. This shift highlights the difference between the diffractograms, confirming that they represent distinct phases. The second phase (AlLi) also begins to form with short milling times, and its intensity does not interfere with the aluminum and $Al_{8.9}Li_{1.1}$ phases. The peak located at an angle of 40.067 degrees (diffractogram b) corresponds to the AlLi phase. As milling time increases, the peaks of both AlLi and $Al_{8.9}Li_{1.1}$ phases become broader due to the smaller particle sizes. This is a

typical characteristic of the mechanical alloying technique, where extended milling times tend to partially amorphized the materials; therefore, on this occasion with the programmed milling time of 3 h, a nanocrystalline structure is formed. The difference in theoretical values (0.104 degrees) confirms the formation of both phases (AlLi and $Al_{8.9}Li_{1.1}$). The milling time was relatively short (30 min) to initiate phase formation from the Al and Li metals used in this study. All experimental runs with an 80:20 weight ratio of Al to Li yielded reproducible results. The AlLi and $Al_{8.9}Li_{1.1}$ phases in these proportions were considered for hydrogen generation reactions with water. The diffractogram obtained after 30 min of milling does not indicate the complete formation of the alloy. To verify whether aluminum had alloyed with lithium, the product obtained after 30 min of milling was reacted with water to generate hydrogen, and the byproduct was analyzed by X-ray diffraction. The result showed the presence of metallic aluminum. With longer programmed milling times, the AlLi and $Al_{8.9}Li_{1.1}$ phases continued to form through repeated collisions between the milling media and the container walls until the complete combination of aluminum and lithium. Another characteristic is the width of the main peaks. The peak observed at 30 min is narrower because some aluminum particles of a certain size have not yet fully reacted with lithium. This contrasts with the peak obtained after 3 h, where the transformation of aluminum and lithium has been fully completed, resulting in the formation of the AlLi and $Al_{8.9}Li_{1.1}$ phases. As a result of this process, very small particles are formed, leading to broader peaks, as shown in diffractogram (e). Equations (1) and (2) illustrate the reactions occurring inside the container during the milling process, where aluminum and lithium, after 3 h of milling, are fully combined.

$$Al + Li \rightarrow AlLi \quad (1)$$

$$8.9Al + 1.1Li \rightarrow Al_{8.9}Li_{1.1} \quad (2)$$

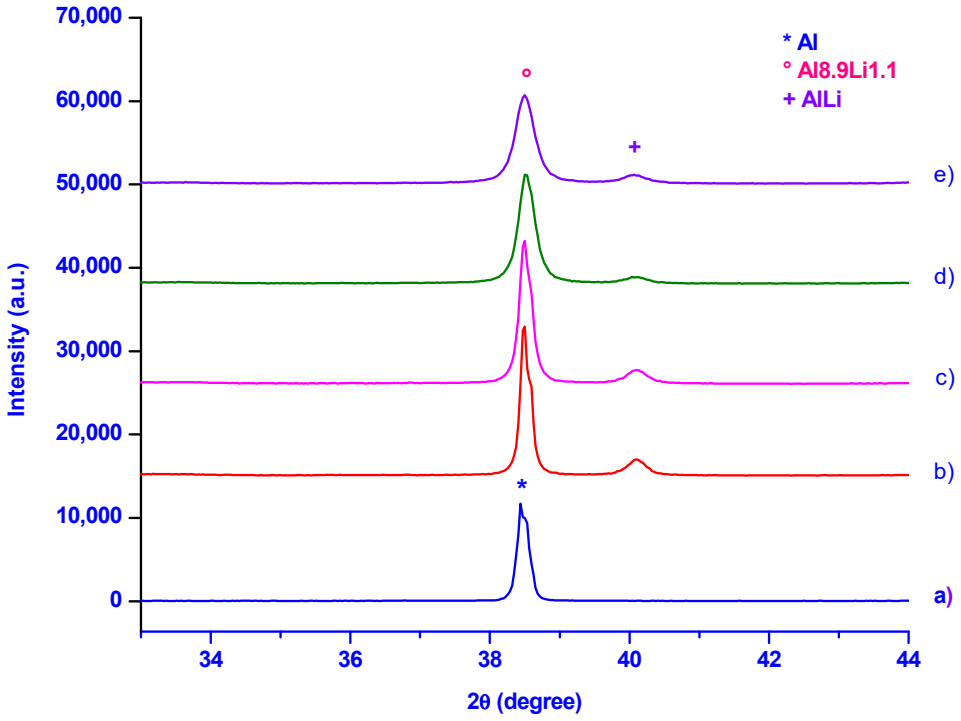

Figure 6. Amplification and comparison between the Al (a) main peak and $Al_{8.9}Li_{1.1}$ and AlLi phases 30 min (b), 1 (c), 2 (d), and 3 h (e) of milling.

Under these conditions, when using lithium at 20% by weight combined with aluminum particles, two phases were obtained. In the diffractograms (Figure 5), no other phases were identified.

The phases identified through their corresponding diffractograms, based on milling times, were reacted with distilled water to produce hydrogen. Table 1 shows the parameters used for hydrogen generation, such as milling times, the weight of the material used in the reactions, and the volume of hydrogen generated. The first column lists the milling times, programmed from 30 min to 10 h. The second column indicates the sample weights, which were kept constant at 100 mg, and the third column shows the volume of hydrogen generated as a function of milling time. The first series of reactions, considering the material obtained after 30 min of milling and reacted with water under normal conditions, were carried out. On this occasion, the volume of hydrogen generated was 44 mL. It is assumed that during this milling time, the Al and Li material had begun forming the AlLi and $Al_{8.9}Li_{1.1}$ phases, which reacted with water to produce clean hydrogen, as no other gas was detected by gas chromatography. Under these milling conditions, the aluminum did not react with water, likely due to its particle size. In these conditions, the presence of aluminum particles was mixed with the AlLi phases that had formed, as demonstrated by the diffraction pattern of the by-product obtained after the reaction with water. The hydrolysis reactions between the AlLi and $Al_{8.9}Li_{1.1}$ phases and water were conducted under laboratory conditions, specifically at a temperature of 20 °C, without the addition of any additives or catalysts to generate hydrogen. The particle size of the aluminum also influenced the reaction, as observed in the SEM results. Relatively large particles were still visible after 30 min of milling (Figure 3A), indicating a limit in aluminum particle size that remained too large to fully react with water and thus obtain the maximum volume of hydrogen. Given the unreacted aluminum particles under these conditions, the milling time was increased to 1 h. This resulted in a 3.4-times increase in hydrogen volume compared to the previous value obtained after 30 min. At this point, the average volume of hydrogen produced was 150 mL. As the milling time increased, the hydrogen volume also increased, reaching a maximum of 170 mL after 3 h of milling. At this stage, the particle size was homogeneous, allowing the material to fully react and produce the maximum gas volume. To confirm that this represented the maximum volume (or plateau) of hydrogen generation, additional milling times of 5 and 10 h were tested. However, the volume of hydrogen remained constant as that obtained after 3 h of milling, which indicates that this time was optimal to produce the maximum volume of hydrogen. These values were reproducible, and based on these results, the high-energy mechanical milling process was standardized at 3 h to minimize energy consumption and save time.

Table 1. Hydrogen generation from AlLi phases and water as a function of milling time.

Milling Time (h)	AlLi-$Al_{8.9}Li_{1.1}$ Phases (mg)	Vol. of H_2 (mL)
0.5	100	44 ± 2.17
1	100	150 ± 2.84
2	100	165 ± 4.54
3	100	170 ± 0.07
5	100	170 ± 0.08
10	100	170 ± 0.05

Figure 7 shows the clean hydrogen volume versus the weight of the material used. Each point represents the amount of material that reacted with water to generate hydrogen. The quantities of the powders for the reactions ranged from 20 to 200 mg. These small amounts were chosen because the reaction between the AlLi material and water occurred quickly and vigorously. However, the curve shows a linear trend in hydrogen production relative to the amount of material used. The R-value is acceptable as all points pass through the line, indicating a proportional relationship between the amount of AlLi and $Al_{8.9}Li_{1.1}$ material and hydrogen production. This is significant because, in principle, any amount of material can be reacted with water to produce large volumes of hydrogen. Under these experimental conditions, the reactions between the AlLi and $Al_{8.9}Li_{1.1}$ phases and water

were conducted at ambient conditions without the addition of additives or catalysts to initiate the hydrogen generation process.

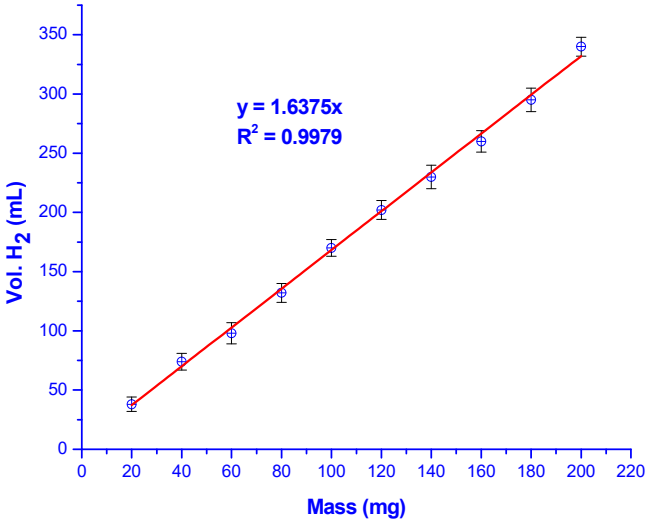

Figure 7. Linear trend in hydrogen generation as a function of weight material.

Figure 8 shows the kinetics of hydrogen generation when the phases (AlLi and $Al_{8.9}Li_{1.1}$) react with water as a function of reaction time. Upon contact with water, the reaction started rapidly, and hydrogen was produced immediately. The volume of hydrogen was measured at specific time intervals, beginning at 20 s and continuing until the reaction was completed, after 10 min. The kinetics of hydrogen generation under ambient conditions are considered relatively fast, as the materials reacted completely without the addition of any catalyst. As shown in the graph, after 1 min of reaction, more than 50% of the total hydrogen volume had already been generated. After 2 min, the reaction rate slowed because most of the material had already reacted, reducing the hydrogen production rate until the total volume was reached. Since the reaction is exothermic, the temperature in the system began to decrease relative to the environment during this time interval. As a result, the heat generated was not sustained as it was at the start, leading to a slower reaction rate, which delayed the final hydrogen production. In another series of experiments, hydrogen was measured up to 30 min after the reaction started and the hydrogen volume remained constant to that measured after 10 min. Therefore, the volume of hydrogen (170 mL) was the same for 30 min; that is, the material reacted in a short time.

The reactions that occur between Al-20Li material milled 3 h and water in hydrogen generation are represented in Equations (3)–(5).

$$2Li + 2H_2O \rightarrow 2LiOH + H_2 \quad (3)$$

$$2Al + 6H_2O \rightarrow 2Al(OH)_3 + 3H_2 \quad (4)$$

$$LiOH + 2Al(OH)_3 + 2H_2O \rightarrow LiAl_2(OH)_7{\cdot}2H_2O \quad (5)$$

These reactions may also occur in the system almost instantaneously. For example, the $Al(OH)_3$ by-product is formed in a hydrolytic process, which reacts with LiOH and water to produce the final by-product $LiAl_2(OH)_7{\cdot}2H_2O$. This by-product was not found mixed with any other phase, as demonstrated by its diffraction pattern. When the maximum volume of hydrogen was reached as a function of milling time at 3, 5, and 10 h, which showed a constant value, the efficiency of hydrogen generation between the phases (AlLi and $Al_{8.9}Li_{1.1}$) and distilled water under laboratory conditions—at room temperature (20 °C)—was determined. In all tests conducted at different milling times from 3 h, the hydrogen volume was 1700 mL/g of material. Based on these results, the efficiency of hydrogen production was 100%, as the material reacted completely. To confirm whether the efficiency matched the reported value, the by-product obtained after the reaction was

analyzed by X-ray diffraction to check if the phases (AlLi and $Al_{8.9}Li_{1.1}$) had fully reacted. The results from these analyses showed the presence of only one by-product (Figure 9), confirming that hydrogen had been completely generated. This indicates that the process of obtaining clean hydrogen under these conditions was 100% efficient, meaning both phases reacted fully to generate a consistent hydrogen volume after 3 h. Additionally, to determine aluminum's contribution to hydrogen production from both phases, considering the 20% lithium used, lithium alone was reacted with water under identical laboratory conditions. Five reactions were performed, with an average lithium sample weight of 0.1 g, yielding an average hydrogen volume of 155 mL, or 1550 mL/g; using this result, the volume of hydrogen contributed by aluminum was calculated. According to these results, 1700 mL of hydrogen was generated per gram from the AlLi and $Al_{8.9}Li_{1.1}$ phases. In this study, the concentration of aluminum was 80% by weight; thus, aluminum contributed 1390 mL of hydrogen, while lithium generated 20%, or 310 mL/g of material. This combination is notable because aluminum particles typically do not react with water under these conditions due to the oxide layer formed on their surface. However, when aluminum is mixed with lithium through mechanical milling, the phases react and generate a significant volume of hydrogen. Table 2 highlights various studies that have used aluminum as a base to generate hydrogen through different methods and its combination with elements such as Ga, In, Si, Li, C, Bi, Zn, Mg, and Fe. It also includes hydrogen production by mixing aluminum with chemical compounds such as NaCl, $SnCl_2$, and Bi_2O_3 to form composites or intermetallic compounds, which were activated through the mechanical milling process. The milling times in these studies ranged from several minutes to 19 h [52–56]. The reactions to generate hydrogen were carried out under various temperature conditions, ranging from −10 °C to 80 °C, depending on the aluminum combination and the solution used. Most studies employed water as the reaction medium. In addition to water, another solution considered for hydrolysis to produce hydrogen has been an alkaline solution [57–59]. Similarly, aluminum has been combined with lithium to generate hydrogen through thermal processes at high temperatures [60,61]. Others have combined aluminum and lithium to react with different elements and compounds [62]. Table 2 presents the results reported for hydrogen generation, using aluminum as the base element to form various alloys and compounds, along with their respective reactions, experimental conditions, and the volume of hydrogen generated. It also includes the experimental conditions and hydrogen generation results from the aluminum–lithium binary system phases, AlLi and $Al_{8.9}Li_{1.1}$, obtained by mechanical milling and reported in this work.

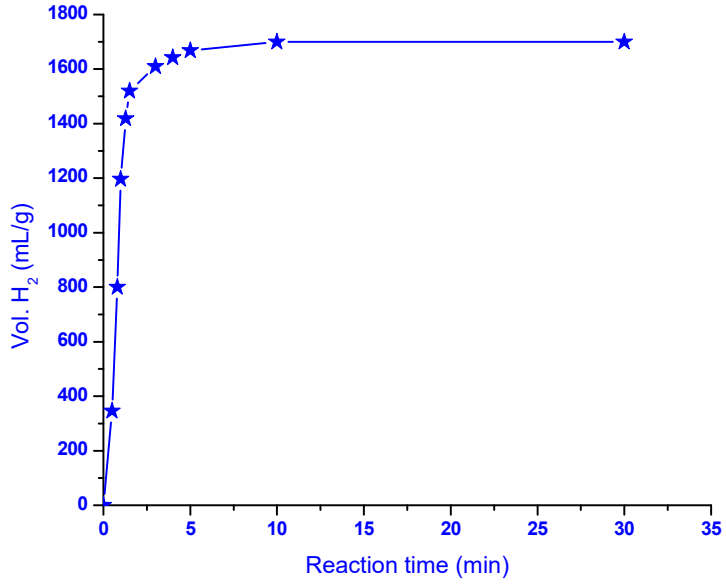

Figure 8. Kinetics during hydrolysis reaction in hydrogen production.

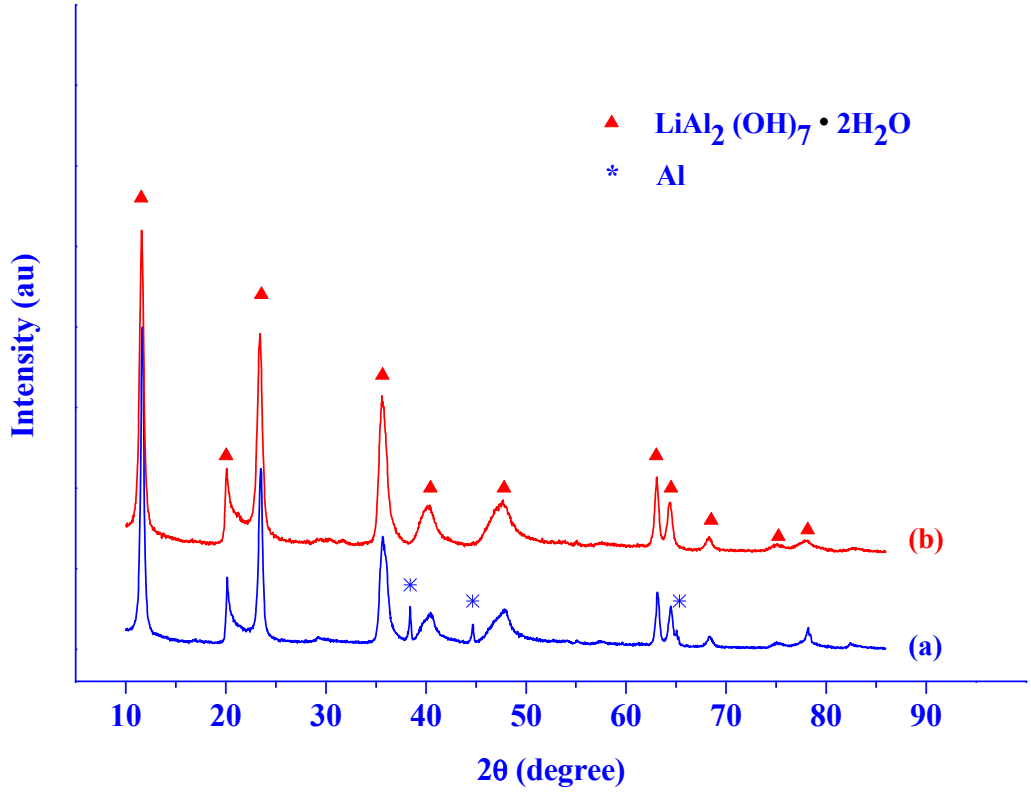

Figure 9. Diffractograms of by-product at 30 min (a) and 3 h (b) of milling.

Table 2. Various reported methods for hydrogen production involving the combination of aluminum with other elements and compounds, along with the conditions used in this work.

Compound or System	Method and Time	Temp. (°C)	Reaction Medium	Hydrogen (mL/g)	Ref.
GaInAl	MM (3 min)	0	H_2O	1280	[52]
AlGaInSnCl$_2$-Bi$_2$O$_3$	MM (3 h)	25	H_2O	1172	[53]
AlSiCBi-NaCl	MM (15 h)	70	H_2O	730	[54]
Al-NaCl	MM (5 h)	70	H_2O	1641	[55]
Al-(NaCl)	MM (19 h)	80	Hot H_2O	1270	[56]
Al-Ni	MM (5 h)	70	Alkaline sol	1350	[57]
Al-GaInZn	MM (10 min)	−10	Alkaline sol	1056	[58]
Al-Mg-Fe	MM (4 h)	25	Alkaline sol	1013	[59]
Al-20Li	Thermal	700	H_2O	1039	[60]
Al-20Li	Thermal	700	H_2O	1164	[61]
Al-Li-InZn	MM (15 h)	25	H_2O	1245	[47]
Al-Li-(NaCl)	MM (15 h)	25	H_2O	1245	[62]
Al-20Li	MM (3 h)	20	H_2O	1700	This work

The table presents various investigations with different experimental conditions for generating hydrogen through material reactions. In these studies, the hydrogen volume varied, with reported values ranging from 730 to 1641 mL/g when aluminum was combined with other elements and compounds. In contrast, the hydrogen volume reported from combining certain elements with lithium ranged from 1039 to 1245 mL/g. It is important to note that the methods used in these studies differ in several parameters from those employed in this work. Under our experimental conditions, which were conducted in a straightforward manner, the hydrogen volume reached 1700 mL/g, and this value was reproducibly achieved. The ease of obtaining the AlLi and $Al_{8.9}Li_{1.1}$ phases, which reacted with distilled water to generate hydrogen, is significantly different from that reported in other studies listed in Table 2, particularly methods that used lithium in combination

with aluminum and other compounds. A notable advantage was the use of short milling times, unlike those listed in the table, such as 15 h of milling or the thermal method. Both approaches generated smaller hydrogen volumes compared to this work. Figure 9 represents the diffractograms of the by-product obtained after the reaction between the AlLi and $Al_{8.9}Li_{1.1}$ phases and water during hydrogen generation for milling times of 30 min and 3 h, (a) and (b), respectively. In diffractogram (a), two phases were identified: the corresponding by-product ($LiAl_2(OH)_7{\cdot}2H_2O$) and aluminum. The presence of aluminum indicates that after 30 min of milling, the aluminum had not yet fully combined. This result explains the smaller volume of hydrogen produced during 30 min of milling time, meaning that aluminum particles remained at a size that did not fully react with water. Additionally, this milling time and its corresponding analysis revealed the formation of the AlLi and $Al_{8.9}Li_{1.1}$ phases. Diffractogram (b) shows the by-product obtained after hydrogen generation from the reaction of the AlLi and $Al_{8.9}Li_{1.1}$ phases with water. The lithium aluminum hydroxide hydrate phase ($LiAl_2(OH)_7{\cdot}2H_2O$) was identified using PDF card 31-0704. All peaks observed in the diffractogram correspond to this phase. It is important to note that the combination of the two phases during the reaction resulted in only one by-product being formed, as no other phase appeared in the diffractogram. Since the by-product is a single compound, it can be used directly in subsequent chemical processes. Through diffraction analysis, the efficiency of hydrogen production was verified, showing that the reaction of the material with water was complete, providing 100% efficiency.

In this work, the mechanical milling method was highly favorable for producing the AlLi alloy, as the material synthesis was completed in just 3 h, resulting in nanometric-sized powders that reacted with water efficiently and rapidly. The various processes occurring during alloying allowed for the rapid fusion of Al and Li metals without requiring significant energy input, unlike other methods that involve reaching their respective melting points and transforming them into liquid phases. The mechanical alloying technique avoids these conditions. Moreover, since both metals are considered soft, alloy preparation is further facilitated. Throughout the hydrogen production process, no greenhouse gases were produced. However, Al and Li metals must be handled in an inert atmosphere to prevent oxide formation during preparation and milling, because these metals react quickly with environmental components.

4. Conclusions

Two phases of AlLi were successfully prepared, which react easily with water to produce clean hydrogen. The mechanical alloying method proved to be very suitable for synthesizing these phases. The AlLi and $Al_{8.9}Li_{1.1}$ phases were formed using 20 wt% lithium and aluminum. No additives were used in the preparation of the materials from aluminum and lithium through mechanical milling. Milling media of the appropriate diameter were used, causing strong impacts between the container walls and the material, resulting in the rapid formation of AlLi phases. The formation of these phases begins at relatively short milling times, with the complete combination of both metals achieved in 3 h. The kinetics of hydrogen production between the AlLi and $Al_{8.9}Li_{1.1}$ phases and water were fast, vigorous, and exothermic, which could be controlled by adding water gradually until the desired volume was reached. The volume of hydrogen produced was 1700 mL/g of material. Hydrogen generation was performed under ambient conditions without the addition of catalysts, achieving 100% efficiency. The contribution of aluminum mixed with 20% lithium by weight in hydrogen production was particularly significant, reaching 82%. Hydrated lithium aluminum hydroxide ($LiAl_2(OH)_7{\cdot}2H_2O$) was obtained as the only by-product, confirmed by XRD, and this hydroxide has important applications. Additionally, the reaction between the AlLi phases and water, generating the maximum volume of hydrogen, was completed. Alloy synthesis from Al and Li using the mechanical alloying technique opens the possibility of producing clean hydrogen on a larger scale using water as a key element in fuel cells, especially in zero-emission (ZECO2) transportation. This method proves to be highly effective in obtaining hydrogen in a direct, simple, and viable

way. Throughout the process used in this work to generate hydrogen, unlike traditional methods, no greenhouse gas emissions were produced. According to the results and under the conditions carried out in this research, these compounds (AlLi) can serve as energy storage; in the same way, the hydrogen produced does not require prior purification and therefore can be used directly in fuel cells, and in the near future, it can also be used as a possible substitute for fossil fuels.

Author Contributions: J.L.I.-G.: research, project planning, methodology, writing—original draft, and writing—review and editing. D.L.A.-A.: research, methodology, and XRD analysis. The authors contributed to the discussion of the results presented and editing. All authors have read and agreed to the published version of the manuscript.

Funding: This research received no external funding.

Data Availability Statement: No additional data was created.

Acknowledgments: The authors thank the XRD and SEM staff as well as the technicians of the Chemistry Department for their valuable support in carrying out the corresponding analyses.

Conflicts of Interest: The authors declare no conflicts of interest.

References

1. Razm, R.; Lin, N. Hydrogen demand potential and economics for heavy-duty vehicles and fracking: Sustainable development. *Int. J. Hydrogen Energy* **2024**, *53*, 1404–1420. [CrossRef]
2. Da Silva Veras, T.; Simonato Mozer, D.; Da Costa Rubim Messeder Dos Santos, A.; Da Silva, C. Hydrogen: Trends, production and characterization of the main process worldwide. *Int. J. Hydrogen Energy* **2017**, *42*, 2018–2033. [CrossRef]
3. Pashchenko, D.; Nikitin, M. Forging furnace with thermochemical waste-heat recuperation by natural gas reforming: Fuel saving and heat balance. *Int. J. Hydrogen Energy* **2021**, *46*, 100–109. [CrossRef]
4. Pashchenko, D. Industrial furnaces with thermochemical waste-heat recuperation by coal gasification. *Energy* **2021**, *221*, 119864. [CrossRef]
5. Dincer, I. Green methods for hydrogen production. *Int. J. Hydrogen Energy* **2012**, *37*, 1954–1971. [CrossRef]
6. Nikolaidis, P.; Poullikkas, A. A comparative overview of hydrogen production processes. *Renew. Sustain. Energy Rev.* **2017**, *67*, 597–611. [CrossRef]
7. Franzoni, F.; Milani, M.; Montorsi, L.; Golovitchev, V. Combined hydrogen production and power generation from aluminum combustion with water: Analysis of the concept. *Int. J. Hydrogen Energy* **2010**, *35*, 1548–1559. [CrossRef]
8. Lokesh, S.; Srivastava, R. CuAl layered double hydroxide as a highly efficient electrocatalyst for the electrolysis of water into hydrogen and oxygen fuels. *Int. J. Hydrogen Energy* **2023**, *48*, 35–50. [CrossRef]
9. Escobar-Alarcón, L.; Iturbe-García, J.L.; González-Zavala, F.; Solís-Casados, D.A.; Pérez-Hernándeze, R.; Haro-Poniatowski, E. Hydrogen production by ultrasound assisted liquid laser ablation of Al, Mg and Al-Mg alloys in water. *Appl. Surf. Sci.* **2019**, *479*, 189–196. [CrossRef]
10. Escobar-Alarcón, L.; Iturbe-García, J.L.; González-Zavala, F.; Solís-Casados, D.A.; Pérez-Hernándeze, R.; Haro-Poniatowski, E. Hydrogen production by laser irradiation of metals in water under an ultrasonic field: A novel approach. *Int. J. Hydrogen Energy* **2019**, *44*, 1579–1581. [CrossRef]
11. Iturbe-García, J.L.; Peña-Ferreyra, D.L. Alternative method for generating hydrogen through high-energy mechanical milling using magnesium and methanol. *Int. J. Hydrogen Energy* **2020**, *45*, 28383–28393. [CrossRef]
12. Shanmugam, V.; Neuberg, S.; Zapf, R.; Pennemann, H.; Kolb, G. Hydrogen production over highly active Pt based catalyst coatings by steam reforming of methanol: Effect of support and co-support. *Int. J. Hydrogen Energy* **2020**, *45*, 1658–1670. [CrossRef]
13. Deguchi, S.; Kobayashi, N.; Isu, N.; Ito, M. Direct production of hydrogen-rich gas and/or pure-hydrogen with high-pressure from alcohol/water/metal-powder mixture at low processing temperature. *Int. J. Hydrogen Energy* **2020**, *45*, 2513–2526. [CrossRef]
14. Li, J.; Mei, X.; Zhang, L.; Yu, Z.; Hu, X. A comparative study of catalytic behaviors of Mn, Fe, Co, Ni, Cu and Zn–Based catalysts in steam reforming of methanol, acetic acid and acetone. *Int. J. Hydrogen Energy* **2020**, *45*, 3815–3832. [CrossRef]
15. Naga, M.; Balaji, K.R.; Dhathathreyan, K.S. Palladium nanoparticles as hydrogen evolution reaction (HER) electrocatalyst in electrochemical methanol reformer. *Int. J. Hydrogen Energy* **2016**, *41*, 46–51. [CrossRef]
16. Rednyk, V.; Johánek, I.; Khalakhan, M.; Dubau, V.M. Methanol oxidation on sputter-coated platinum oxide catalysts. *Int. J. Hydrogen Energy* **2016**, *41*, 265–275. [CrossRef]
17. Eisa, T.; Mohamed, H.O.; Choi, Y.J.; Park, S.G.; Chae, K.J. Nickel nanorods over nickel foam as standalone anode for direct alkaline methanol and ethanol fuel cell. *Int. J. Hydrogen Energy* **2020**, *45*, 5948–5959. [CrossRef]
18. Yavor, Y.; Goroshin, S.; Bergthorson, J.M.; Frost, D.L.; Stowe, R.; Ringuette, S. Enhanced hydrogen generation from aluminum water reactions. *Int. J. Hydrogen Energy* **2013**, *38*, 14992–15002. [CrossRef]

19. Wang, H.Z.; Leung, D.Y.C.; Leung, M.K.H.; Ni, M. A review on hydrogen production using aluminum and aluminum alloys. *Renew. Sustain. Energy Rev.* **2009**, *13*, 845–853. [CrossRef]
20. Alinejad, B.; Mahmoodi, K. A novel method for generating hydrogen by hydrolysis of highly activated aluminum nanoparticles in pure water. *Int. J. Hydrogen Energy* **2009**, *34*, 7934–7948. [CrossRef]
21. Kumar, D.; Muthukumar, K. A review of unique aluminum–water based hydrogen production options. *Energy Fuels* **2021**, *35*, 1024–1040. [CrossRef]
22. Etminanbakhsh, M.; Allahkaram, S.R. Reaction of aluminum particles with superheated steam to generate hydrogen gas as a readily usable clean fuel. *Fuel* **2023**, *332 Pt 1*, 126011. [CrossRef]
23. Dincer, I.; Acar, C. Review and evaluation of hydrogen production methods for better sustainability. *Int. J. Hydrogen Energy* **2015**, *40*, 11094–11111. [CrossRef]
24. Grosjean, M.H.; Zidoune, M.; Roué, L.; Huot, J.Y. Hydrogen production via hydrolysis reaction from ball-milled Mg-based materials. *Int. J. Hydrogen Energy* **2006**, *31*, 109–119. [CrossRef]
25. Wang, H.; Ma, H.; Jin, Z.; Shi, J.; Zhang, Z.; Wei, C.; Gao, Q.; Hou, G. Sn-free Al-based on-demand hydrogen production materials for easy recycling. *Int. J. Hydrogen Energy* **2024**, *49 Pt A*, 1332–1343. [CrossRef]
26. Wang, W.; Chen, D.M.; Yang, K. Investigation on microstructure and hydrogen generation performance of Al-rich alloys. *Int. J. Hydrogen Energy* **2010**, *35*, 12011–12019. [CrossRef]
27. Nie, H.; Zhang, S.; Schoenitz, M.; Dreizin, E.L. Reaction interface between aluminum and water. *Int. J. Hydrogen Energy* **2013**, *38*, 11222–11232. [CrossRef]
28. Soler, L.; Macanas, J.; Muñoz, M.; Casado, J. Aluminum and aluminum alloys as sources of hydrogen for fuel cell applications. *J. Power Sources* **2007**, *169*, 144–149. [CrossRef]
29. Ilyukhina, A.V.; Ilyukhin, A.S.; Shkolnikov, E.I. Hydrogen generation from water by means of activated aluminum. *Int. J. Hydrogen Energy* **2012**, *37*, 16382–16387. [CrossRef]
30. Parmuzina, A.V.; Kravchenko, O.V. Activation of aluminum metal to evolve hydrogen from water. *Int. J. Hydrogen Energy* **2008**, *33*, 3073–3076. [CrossRef]
31. Ilyukhina, A.V.; Kravchenko, O.V.; Bulychev, B.M.; Shkolnikov, E.I. Mechanochemical activation of aluminum with gallams for hydrogen evolution from water. *Int. J. Hydrogen Energy* **2010**, *35*, 1905–1910. [CrossRef]
32. Ziebarth, J.T.; Woodal, J.M.; Kramer, R.A.; Choi, G. Liquid phase-enabled reaction of Al-Ga and Al-Ga-In-Sn alloys with water. *Int. J. Hydrogen Energy* **2011**, *36*, 5271–5279. [CrossRef]
33. Wang, W.; Zhao, X.M.; Chen, D.M.; Yang, K. Insight into the reactivity of Al-Ga-In-Sn alloy with water. *Int. J. Hydrogen Energy* **2012**, *37*, 2187–2194. [CrossRef]
34. Wang, W.; Chen, W.; Zhao, X.M.; Chen, D.M.; Yang, K. Effect of composition on the reactivity of Al-rich alloys with water. *Int. J. Hydrogen Energy* **2012**, *37*, 18672–18678. [CrossRef]
35. Yuan, B.; Tan, S.; Liu, J. Dynamic hydrogen generation phenomenon of aluminum fed liquid phase Ga-In alloy inside NaOH electrolyte. *Int. J. Hydrogen Energy* **2016**, *41*, 1453–1459. [CrossRef]
36. Yang, X.H.; Yuan, B.; Liu, J. Metal substrate enhanced hydrogen production of aluminum fed liquid phase Ga-In alloy inside aqueous solution. *Int. J. Hydrogen Energy* **2016**, *41*, 6193–6199. [CrossRef]
37. Kravchenko, O.V.; Semenenko, K.N.; Bulychev, B.M.; Kalmykov, K.B. Activation of aluminum metal and its reaction with water. *J. Alloys Compd.* **2005**, *397*, 58–62. [CrossRef]
38. Deng, Z.Y.; Tang, Y.B.; Zhu, L.L.; Sakka, Y.; Ye, J. Effect of different modification agents on hydrogen-generation by the reaction of Al with water. *Int. J. Hydrogen Energy* **2010**, *35*, 9561–9568. [CrossRef]
39. Huang, X.; Gao, T.; Pan, X.; Wei, D.; Lv, C.; Qin, L.; Huang, Y. A review: Feasibility of hydrogen generation from the reaction between aluminum and water for fuel cell applications. *J. Power Sources* **2013**, *229*, 133–140. [CrossRef]
40. Gai, W.Z.; Wang, L.Y.; Lu, M.Y.; Deng, Z.Y. Effect of low concentration hydroxides on Al hydrolysis for hydrogen production. *Energy* **2023**, *268*, 126731. [CrossRef]
41. López-Miranda, J.L.; Rosas, G. Hydrogen generation by aluminum hydrolysis using the Fe_2Al_5 intermetallic compound. *Int. J. Hydrogen Energy* **2016**, *41*, 4054–4059. [CrossRef]
42. Khzouz, M.; Gkanas, I.E.; Girella, A.; Statheros, T.; Milanese, C. Sustainable hydrogen production via LiH hydrolysis for unmanned air vehicle (UAV) applications. *Int. J. Hydrogen Energy* **2020**, *45*, 5384–5394. [CrossRef]
43. Liu, Y.; Wang, X.; Liu, H.; Dong, Z.; Li, S.; Ge, H.; Yan, M. Effect of salts addition on the hydrogen generation of Al-LiH composite elaborated by ball milling. *Energy* **2015**, *89*, 907–913. [CrossRef]
44. Chen, X.; Zhao, Z.; Hao, M.; Wang, D. Hydrogen generation by splitting water with Al-Li alloys. *Int. J. Energy Res.* **2013**, *37*, 1624–1634. [CrossRef]
45. Rosenband, V.; Gany, A. Application of activated aluminum powder for generation of hydrogen from water. *Int. J. Hydrogen Energy* **2010**, *35*, 10898–10904. [CrossRef]
46. Chen, X.; Zhao, Z.; Liu, X.; Hao, M.; Chen, A.; Tang, Z. Hydrogen generation by the hydrolysis reaction of ball-milled aluminium-lithium alloys. *J. Power Sources.* **2014**, *254*, 345–352. [CrossRef]
47. Fan, M.Q.; Liu, S.; Wang, C.; Chen, D.; Shu, K.Y. Hydrolytic hydrogen generation using milled aluminum in water activated by Li, In, and Zn additives. *Fuel Cells* **2011**, *12*, 642–648. [CrossRef]

48. Elitzur, S.; Rosenband, V.; Gany, A. Study of hydrogen production and storage based on aluminum-water reaction. *Int. J. Hydrogen Energy* **2014**, *39*, 6328–6334. [CrossRef]
49. Sampayo Palma, A.; Iturbe-García, J.L.; López-Muñoz, B.E.; Sandoval Jiménez, A. MgAl alloy synthesis, characterization and its use in hydrogen storage. *Int. J. Hydrogen Energy* **2010**, *35*, 12120–12124. [CrossRef]
50. Iturbe-García, J.L.; Bonifacio Martínez, J.; Granados Correa, F.; López-Muñoz, B.E. Behavior of a hydrotalcite type material obtained from MgAl alloy for CO_2 adsorption. *Appl. Clay Sci.* **2019**, *183*, 105296. [CrossRef]
51. Wang, s.; Dou, T.; Li, Y.; Zhang, Y.; Li, X.; Yan, Z. Synthesis, characterization, and catalytic properties of stable mesoporous molecular sieve MCM-41 prepared from zeolite mordenite. *J. Solid State Chem.* **2004**, *177*, 4800–4805. [CrossRef]
52. Ilyukhina, A.V.; Kravchenko, O.V.; Bulychev, B.M. Studies on microstructure of activated aluminum and its hydrogen generation properties in aluminum/water reaction. *J. Alloys Compd.* **2017**, *690*, 321–329. [CrossRef]
53. Guan, X.; Zhou, Z.; Luo, P.; Wu, F.; Dong, S. Hydrogen generation from the reaction of Al-based composites activated by low-melting-point metals/oxides/salts with water. *Energy* **2019**, *188*, 116107. [CrossRef]
54. Mahmoodi, K.; Alinejad, B. Enhancement of hydrogen generation rate in reaction of aluminum with water. *Int. J. Hydrogen Energy* **2010**, *35*, 5227–5232. [CrossRef]
55. Irankhah, A.; Fattahi, S.M.S.; Salem, M. Hydrogen generation using activated aluminum/water reaction. *Int. J. Hydrogen Energy* **2018**, *43*, 15739–15748. [CrossRef]
56. Razavi Tousi, S.S.; Szpunar, J.A. Effect of addition of water-soluble salts on the hydrogen generation of aluminum in reaction with hot water. *J. Alloys Compd.* **2016**, *679*, 364–374. [CrossRef]
57. Ho, C.Y.; Huang, C.H. Enhancement of hydrogen generation using waste aluminum cans hydrolysis in low alkaline de-ionized water. *Int. J. Hydrogen Energy* **2016**, *41*, 3741–3747. [CrossRef]
58. Dudoladov, A.; OBuryakovskaya, O.A.; Vlaskin, M.S.; Zhuk, A.Z.; Shkolnikov, E.I. Generation of hydrogen by aluminum oxidation in aqueous solutions at low temperatures. *Int. J. Hydrogen Energy* **2016**, *41*, 2230–2237. [CrossRef]
59. Wang, C.; Yang, T.; Liu, Y.; Ruan, J.; Yang, S.; Liu, X. Hydrogen generation by the hydrolysis of magnesium-aluminum-iron material in aqueous solutions. *Int. J. Hydrogen Energy* **2014**, *39*, 10843–10852. [CrossRef]
60. Yang, W.; Zhang, T.; Zhou, J.; Shi, W.; Liu, J.; Cen, K. Experimental study on the effect of low melting point metal additives on hydrogen production in the aluminum-water reaction. *Energy* **2015**, *88*, 537–543. [CrossRef]
61. Yang, W.; Zhang, T.; Liu, J.; Wang, Z.; Zhou, J.; Cen, K. Experimental researches on hydrogen generation by aluminum with adding lithium at high temperature. *Energy* **2015**, *93*, 451–457. [CrossRef]
62. Fan, M.Q.; Sun, L.X.; Xu, F.; Mei, D.; Chen, D.; Chai, W.X.; Huang, F.L.; Zhang, Q.M. Microstructure of Al–Li alloy and its hydrolysis as portable hydrogen source for proton-exchange membrane fuel cells. *Int. J. Hydrogen Energy* **2011**, *36*, 9791–9798. [CrossRef]